OCRT Meeting, 5-7 May 2014, Silver Spring, MD, USA.

SWIM: A Semi-analytical ocean color inversion algorithm for optically shallow waters

Lachlan I.W. McKinna*[a,c], P. Jeremy Werdell[b], Peter R.C.S. Fearns[c], Scarla J. Weeks[d], Martina Reichstetter[d], Bryan A. Franz[b], Donald M. Shea[e] and Gene C. Feldman[b]

1. Introduction

Ocean color remote sensing provides synoptic-scale, near-daily observations of marine inherent optical properties (IOPs). Whilst contemporary ocean color algorithms are known to perform well in deep oceanic waters, they have difficulty operating in optically clear, shallow marine environments where light reflected from the seafloor contributes to the water-leaving radiance. The effect of benthic reflectance in "optically shallow" waters is known to adversely affect algorithms developed for optically deep waters [1, 2]. Whilst adapted versions of optically deep ocean color algorithms have been applied to optically shallow regions with reasonable success [3], there is presently no approach that directly corrects for bottom reflectance using existing knowledge of bathymetry and benthic albedo.

To address the issue of optically shallow waters, we have developed a semi-analytical ocean color inversion algorithm: *the Shallow Water Inversion Model* (SWIM). SWIM uses existing bathymetry and a derived benthic albedo map to correct for bottom reflectance using the semi-analytical model of Lee et al [4]. The algorithm was incorporated into the NASA Ocean Biology Processing Group's L2GEN program and tested in optically shallow waters of the Great Barrier Reef, Australia. In-lieu of readily available in situ matchup data, we present a comparison between SWIM and two contemporary ocean color algorithms, the Generalized Inherent Optical Property Algorithm (GIOP) and the Quasi-Analytical Algorithm (QAA).

2. Research objectives

- Develop a shallow water inversion algorithm (SWIM) with depth and benthic albedo as inputs
- Incorporate the algorithm into L2GEN processing software
- Test the algorithm in optically shallow waters of the Great Barrier Reef, Australia
- With the MODIS Aqua time series, compare IOPs and $K_d(488)$ [5] derived using SWIM with values derived by GIOP and QAA

3. Algorithm Structure

SWIM is a forward-inverse type algorithm. A 'forward' semi-analytical model [4] is used to simulate sub-surface remote sensing reflectances, r_{rs}, which are compared within sensor observed values. The internal parameters (IOPs) of the forward model are dynamically varied using a constrained Levenberg-Marquardt non-linear least squares optimization routine. Once the cost function is minimized (i.e. modelled and observed r_{rs} are most similar), SWIM returns the set of optimal IOPs as the 'inverted' solution. If convergence to a solution is not achieved, a product failure (PRODFAIL) flag is returned. Previously developed shallow water inversion algorithms sought to derive IOPs, water column depth, and benthic albedo simultaneously [6]. However such approaches were typically concerned with mapping bathymetry and/or benthic classification using airborne hyperspectral imagery. Conversely, SWIM uses bathymetry and a benthic albedo data as inputs, thereby reducing the number of free parameters in the algorithm. Within this study, an existing high resolution bathymetry [7] map of the Great Barrier Reef has been used. In addition, extensive knowledge of benthic composition [8] has been used to construct a two-class benthic albedo map of 'light' and 'dark' substrate types.

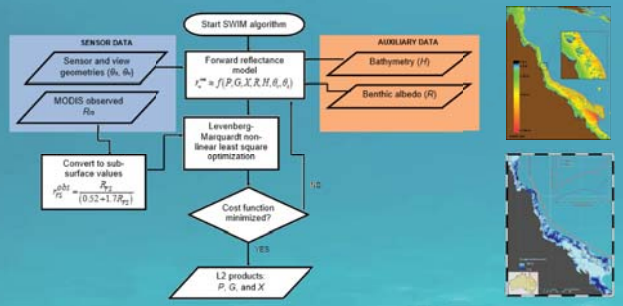

Figure 1: Schematic diagram of the SWIM algorithm. Water column depth and benthic albedo maps are included as auxiliary datasets and are illustrated to the right-hand side of the flow chart. Here, the free parameters P, G, and X, correspond to the absorption coefficient of phytoplankton at 443 nm, $a_\phi(443)$, the absorption coefficient of colored dissolved and detrital matter at 443 nm, $a_{dg}(443)$, and the particulate backscattering coefficient at 443 nm, $b_{bp}(443)$ respectively.

Author affiliations:
[a]NASA Postdoctoral Program Fellow, Ocean Ecology Laboratory (616), Goddard Space Flight Center, Greenbelt, MD, 20771, USA.
[b]Ocean Ecology Laboratory (616), Goddard Space Flight Center, , Greenbelt, MD, 20771, USA.
[c]Department of Imaging and Applied Physics, Curtin University, Perth, WA, 6102, Australia.
[d]School of Geography, Planning and Environmental Management, University of Queensland, QLD, 4702, Australia.
[e]Science Applications International Corporation, Greenbelt, MD, USA.
*Corresponding author email: lachlan.i.mckinna@nasa.gov

4. Test region: the Great Barrier Reef

A sub-set of the northern Great Barrier Reef, Australia was used to demonstrate the SWIM algorithm. The clear shelf waters of this region are on average 18 m deep with a mixed benthos comprising sand, seagrasses and corals. Results in Fig. 2 show that for shallow regions (< 20 m) GIOP and QAA give higher values of $a_t(443)$, $b_{bp}(443)$ and $K_d(488)$ than SWIM. This is further demonstrated using cross-shelf transects (Fig. 3). Difference plots of the transect data (Fig. 4) shows that once a depth of approximately 30 m is reached, SWIM, GIOP and QAA behave similarly. We therefore infer that under the optical conditions of that day (22 May 2009), the combined effect of water column depth and benthic reflectance upon the water-leaving signal diminished, and thus the water became quasi-optically deep, after the depth exceeded 30 m. The differences between SWIM and GIOP/QAA demonstrated here are expected. More specifically, both the GIOP and QAA algorithms assume that the r_{rs} signal is depended only upon IOPs. Thus, unlike SWIM, an increase in sensor-observed r_{rs} due to benthic reflectance is interpreted by GIOP/QAA as increased backscattering and/or absorption which then leads to exaggerated $K_d(488)$.

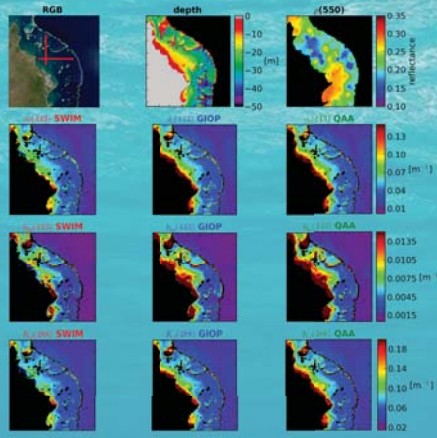

Figure 2: MODIS Aqua test image captured over the northern GBR on 22 May 2009. The top row shows: (I) a RGB image in the top left-hand corner with horizontal (X) and vertical (Y) cross-shelf transects indicated as red lines, (II) the water column depth, and (III) the benthic albedo at 550 nm. The second row shows from left to right values of $a_t(443)$ derived using (I) SWIM, (II) GIOP, and (III) QAA. The third row shows from left to right values of $b_{bp}(443)$ derived using (I) SWIM, (II) GIOP, and (III) QAA. The bottom row shows from left to right values of $K_d(488)$ derived using (I) SWIM, (II) GIOP, and (III) QAA.

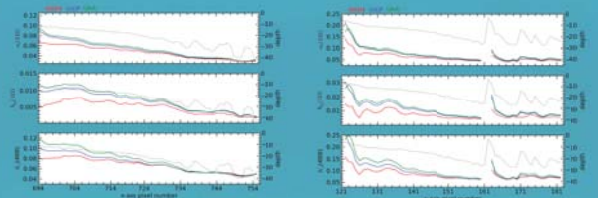

Figure 3: Comparison of $a_t(443)$, $b_{bp}(443)$ and $K_d(488)$ derived using SWIM (red), GIOP (blue) and QAA (green) as cross-shelf water column depth (dotted black) varies. The left and right-hand sides correspond to the X and Y cross-shelf transects depicted in Fig. 2.

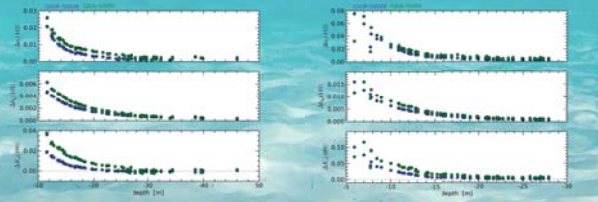

Figure 4: Differences (Δ) between $a_t(443)$, $b_{bp}(443)$ and $K_d(488)$ products derived using: (I) GIOP (blue), and (II) QAA (green) those same products derived using SWIM. These differences are plotted against water column depth. The left and right-hand sides corresponds to data extracted along the X and Y cross-shelf transects depicted in Fig. 2.

5. Time-series comparison

The shallow water (SW) region in Fig 2 and an adjacent offshore deep water (DW) region (depth > 1000 m) were selected for further comparison using the MODIS Aqua time series (2002—2013). Values of $a_t(443)$, $b_{bp}(443)$ and $K_d(488)$ were derived using SWIM, GIOP and QAA from level-1A data and screened for bad values using standard masks and quality control flags. Monthly-averaged data and relative differences were then calculated and are shown in Figs. 5 and 6. Using input bathymetric data, SWIM should mathematically transition into an optically deep model and it was observed that SWIM-derived values were indeed within 10 % of GIOP and QAA values for the DW region. Differences in internal IOP parameterization was inferred to be the reason why SWIM and GIOP/QAA did not converge more closely for the DW region. As expected, SWIM-derived values were consistently lower than GIOP and QAA values through time for the SW region. Differences between SWIM and GIOP/QAA derived products mostly exceeded 10 % for the SW region.

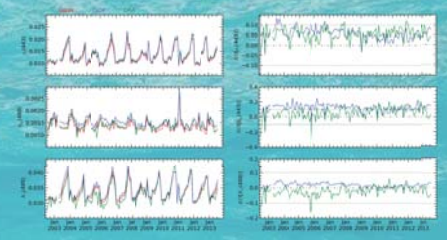

Figure 5: Left-hand side: Monthly means of $a_t(443)$, $b_{bp}(443)$ and $K_d(488)$ for the Deep Water (DW) region retrieved using SWIM (red), GIOP (blue) and QAA (green). Right-hand side: Relative differences between GIOP and SWIM (blue) and QAA and SWIM (green).

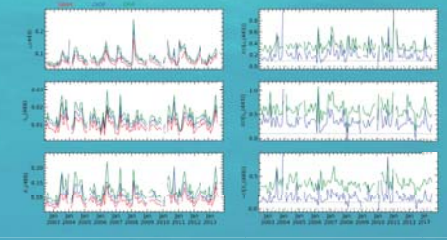

Figure 6: Figure 5: Left-hand side: Monthly means of $a_t(443)$, $b_{bp}(443)$ and $K_d(488)$ for the Shallow Water (SW) region retrieved using SWIM (red), GIOP (blue) and QAA (green). Right-hand side: Relative differences between GIOP and SWIM (blue) and QAA and SWIM (green).

6. Summary

Here we have demonstrated SWIM, an optically shallow ocean color inversion algorithm. The SWIM algorithm is currently an evaluation product within L2GEN processing code and was successfully applied in the Great Barrier Reef, Australia. Comparisons between SWIM and GIOP/QAA indicate the algorithm performs as expected in both deep and shallow waters. SWIM has the potential to enhance research and management of sensitive shallow water environments by complementing existing systems for monitoring water quality and ecosystem health. Further, because SWIM has been developed within the versatile L2GEN processing code it is easily applicable to sensors other than MODIS Aqua and regions outside the Great Barrier Reef.

8. Future work

- Validation and fine tuning of the SWIM algorithm using in situ datasets
- Implementing a tide offset correction procedure
- Extending the SWIM algorithm to other regions with well characterized bathymetry/benthos
- Potential to incorporate SWIM into L2GEN's generalized IOP algorithm framework

References:
1. Zhao et al. (2013), Assessment of satellite-derived diffuse attenuation coefficients and euphotic depths in south Florida coastal waters, *Remote Sens Environ, 131*, 38-50.
2. Cannizzaro and Carder (2006), Estimating chlorophyll a concentrations from remote sensing reflectance in optically shallow waters, *Remote Sens Environ, 101*, 13-24 .
3. Barnes, et al. (2013), MODIS derived spatiotemporal water clarity patterns in optically shallow Florida Keys waters: A new approach to remove bottom contamination, *Remote Sens Environ, 134*, 377-391.
4. Lee et al. (1998), Hyperspectral Remote 1314 Sensing for Shallow Waters. I: A Semianalytical Model, *Appl. Opt.*, 37(27), 6329-6338.
5. Lee et al. (2005), A model for the diffuse attenuation coefficient of downwelling irradiance, *J. Geophys Res: Oceans, 110*(C2), C02016.
6. Dekker, A. G., et al. (2011), Intercomparison of shallow water bathymetry, hydro-optics, and benthos mapping techniques in Australian and Caribbean coastal environments, *Limnol and 1262 Oceanog: Methods, 9*, 396-425.
7. Beaman, 2010), Project 3DGBR: A high-resolution depth model for the Great Barrier Reef and Coral Sea, Marine and Tropical Sciences Research Facility (MTSRF), Project 2.5i.1a Final Report, 13 plus Appendix 11, 225 pp, Cairns, Australia.
8. Pitcher, C. R., et al. (2007), Seabed Biodiversity on the Continental Shelf of the Great Barrier 1371 Reef World Heritage Area, AIMS/CSIRO/QM/QDPI/CRC Reef Research Task Final Report, 329 pp, CSIRO Marine and Atmospheric Research.

Acknowledgements:
This research was generously supported by the Great Barrier Reef Foundation, an Australian Research Council Linkage Project Grant (LP100100342), and a NASA Postdoctoral Program Fellowship at Goddard Space Flight Center administered by Oak Ridge Associated Universities. We thank Sean Bailey, John Wilding and Tommy Owens for their kind support with code development and the handling and processing of large volumes of MODIS Aqua data. Thanks are also extended to Jeffrey Lentz for his kind assistance during this project.